

DTIC FILE COPY

2

TECHNICAL REPORT BRL-TR-3098

**BRL**

AD-A222 591

TEMPERATURE AND OH CONCENTRATIONS  
IN A SOLID PROPELLANT FLAME  
USING ABSORPTION TECHNIQUES

JOHN A. VANDERHOFF  
ANTHONY J. KOTLAR

APRIL 1990

DTIC  
ELECTF  
JUN 12 1990  
S B D

APPROVED FOR PUBLIC RELEASE; DISTRIBUTION UNLIMITED.

U.S. ARMY LABORATORY COMMAND

BALLISTIC RESEARCH LABORATORY  
ABERDEEN PROVING GROUND, MARYLAND

80 08 .11 000

## NOTICES

Destroy this report when it is no longer needed. DO NOT return it to the originator.

Additional copies of this report may be obtained from the National Technical Information Service, U.S. Department of Commerce, 5285 Port Royal Road, Springfield, VA 22161.

The findings of this report are not to be construed as an official Department of the Army position, unless so designated by other authorized documents.

The use of trade names or manufacturers' names in this report does not constitute indorsement of any commercial product.

**UNCLASSIFIED**

REPORT DOCUMENTATION PAGE			Form Approved OMB No. 0704-0188	
<small>Public reporting burden for this collection of information is estimated to average 1 hour per response, including the time for reviewing instructions, searching existing data sources, gathering and maintaining the data needed, and completing and reviewing the collection of information. Send comments regarding this burden estimate or any other aspect of this collection of information, including suggestions for reducing this burden, to Washington Headquarters Service, Directorate for Information Operations and Reports, 1215 Jefferson Davis Highway, Suite 1204, Arlington, VA 22202-4302, and to the Office of Management and Budget, Paperwork Reduction Project (0704-0188), Washington, DC 20503.</small>				
1. AGENCY USE ONLY (Leave blank)		2. REPORT DATE April 1990		3. REPORT TYPE AND DATES COVERED Technical
4. TITLE AND SUBTITLE Temperature and OH Concentrations in a Solid Propellant Flame Using Absorption Techniques			5. FUNDING NUMBERS 1L161102AH43	
6. AUTHOR(S) John A. Vanderhoff Anthony J. Kotlar				
7. PERFORMING ORGANIZATION NAME(S) AND ADDRESS(ES)			8. PERFORMING ORGANIZATION REPORT NUMBER	
9. SPONSORING / MONITORING AGENCY NAME(S) AND ADDRESS(ES) Ballistic Research Laboratory ATTN: SLCBR-DD-T Aberdeen Proving Ground, MD 21005-5066			10. SPONSORING / MONITORING AGENCY REPORT NUMBER BRL-TR-3098	
11. SUPPLEMENTARY NOTES Accepted for presentation at the Army Science Conference, 12-15 Jun3 1990, Durham, NC.				
12a. DISTRIBUTION / AVAILABILITY STATEMENT Approved for public release; distribution unlimited.			12b. DISTRIBUTION CODE	
13. ABSTRACT (Maximum 200 words) Rotationally resolved absorption spectroscopy in the A-X (0,0) vibrational band system of OH around 306.4 nm has been performed to determine the temperature and OH concentration in solid propellant flames. OH is sufficiently well characterized that the spectra can be least squares fitted under a variety of conditions. These conditions include the peculiarities of the experimental setup, instrument response parameters and absorption baseline, as well as the temperature and OH concentration. The multi-parameter least squares fit of the spectra gives values and statistical uncertainties for temperature, OH concentration, and other experimental design parameters. This technique has been applied to a nitramine propellant flame burning in a windowed combustion vessel pressurized with 1.5 MPa nitrogen. A propellant feed mechanism coupled to the combustion vessel extended the data taking time such that good quality OH absorption spectra could be obtained for this transient event. Here the light source was an arc lamp and the detector a spectrometer with an intensified photodiode array. Experimental OH spectral data have been fitted to temperatures ranging from about 2700 to 2000 K with a standard deviation of about 120 K. Together with these temperatures, concentrations that range from about 640 to 250 ppm with a standard deviation of about 6% are also determined. These OH concentration values are consistent with thermochemical equilibrium values for flame temperatures about 80 K below adiabatic and represent the first absolute determinations in a solid propellant flame environment.				
14. SUBJECT TERMS Absorption, Solid Propellant, Combustion, Temperature, Pressure, Flame, OH Concentration, HMX1. (JX) 6			15. NUMBER OF PAGES 24	
			16. PRICE CODE	
17. SECURITY CLASSIFICATION OF REPORT Unclassified	18. SECURITY CLASSIFICATION OF THIS PAGE Unclassified	19. SECURITY CLASSIFICATION OF ABSTRACT Unclassified	20. LIMITATION OF ABSTRACT UL	

NSN 7540-01-280-5500

**UNCLASSIFIED**Standard Form 298 (Rev 2-89)  
Prescribed by ANSI Std Z39-18  
298-102

INTENTIONALLY LEFT BLANK.

## TABLE OF CONTENTS

	<u>PAGE</u>
LIST OF FIGURES . . . . .	v
ACKNOWLEDGEMENT . . . . .	vii
I. INTRODUCTION . . . . .	1
II. EXPERIMENTAL . . . . .	1
III. DATA ANALYSIS . . . . .	3
IV. RESULTS . . . . .	4
V. SUMMARY . . . . .	7
REFERENCES . . . . .	9
APPENDIX . . . . .	11
DISTRIBUTION LIST . . . . .	15



Accession For	
NTIS GRA&I	<input checked="" type="checkbox"/>
DTIC TAB	<input type="checkbox"/>
Unannounced	<input type="checkbox"/>
Justification	
By _____	
Distribution/	
Availability Codes	
Dist	Avail and/or Special
A-1	

INTENTIONALLY LEFT BLANK.

## LIST OF FIGURES

<u>FIGURE</u>	<u>PAGE</u>
1. The optical path for the absorption measurements of propellant burning within a pressurized combustion vessel . . . . .	1
2. A sketch of the major components of the propellant feed mechanism . . .	3
3. An example OH absorption spectrum, taken in a $\text{CH}_4/\text{N}_2\text{O}$ flame at atmospheric pressure . . . . .	4
4. Sample OH absorption data together with the least squares fit for an HMX1 propellant sample burning in 1.5 MPa nitrogen . . . . .	5
5. OH temperatures as a function of distance from the propellant surface . .	6
6. OH concentrations as a function of distance from the propellant surface .	6

INTENTIONALLY LEFT BLANK.



### ACKNOWLEDGEMENT

We thank Dr. Tim Edwards of AFAL for supplying the HMX1 propellant used in this study.

INTENTIONALLY LEFT BLANK.

## I. INTRODUCTION

Understanding a combustion event usually requires knowledge of the temperatures, species involved and their concentration profiles. Thermochemical equilibrium calculations will produce final product species identity and concentration as well as adiabatic flame temperatures; however these results are not very event specific. Information about the detailed chemical pathways from reactants to final products comes from studying the chemically active transient species. These species are generally present in small quantities (<1%) and exist primarily in a zone of small extent: the reaction zone.

The small concentrations of transient combustion species (radicals) renders the use of Raman techniques unattractive for concentration measurements. Non-linear techniques are not considered since they are not simply related to concentration. Laser induced fluorescence (LIF) and absorption have sufficient sensitivity for the detection of the radical species. However, although LIF is a linear technique, it also is not simply related to concentration because of the quenching effects on the excited state which are exacerbated with increasing pressure. Absorption is directly related to concentration and can provide useful information under conditions where a line-of-sight measurement is meaningful.

This paper has a two-fold objective. First, an absorption technique is described which can simultaneously measure temperature and concentration profiles in time varying hostile combustion environments. Second, the viability of this technique is demonstrated by obtaining temperature and OH concentration profiles from a solid propellant flame burning at elevated pressure. This absorption technique is a variation of the method described by Lempert<sup>1</sup>. The present technique, however, has a different light source and detector which allows the OH absorption spectrum to be obtained and analyzed in much more detail as well as allowing different species to be studied with the same experimental setup. A description of the absorption experiment and data analysis is given in the next two sections of the paper.

## II. EXPERIMENTAL

Many investigators have determined OH concentrations from the absorptions in the 306.4 nm system using lamp light sources and a photomultiplier detector. The present arrangement incorporates a high intensity mercury-xenon arc lamp light source but the detector is an intensified photodiode array which can be much more suitable for probing transient combustion processes. As an indication of the sensitivity of the experimental technique, absorptions of 0.15% were readily detectable in a steady state flame environment. The optical path for the absorption measurements of propellant burning within a pressurized combustion vessel is shown on Fig. 1. Two 20 cm focal

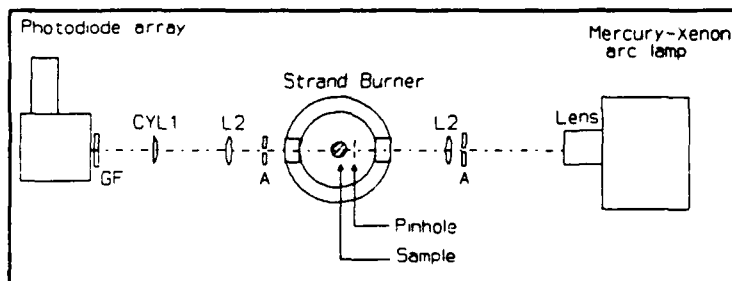


Figure 1 The light path for the optical absorption experiments. The glass filter (GF) was used to eliminate first order light when operating the spectrometer second order; the sample is either a premixed flame or propellant.

length convex lenses (L2) focus and recollimate the light beam from the 1 kw mercury-xenon arc lamp and two apertures and a 0.15 mm pinhole confine the spatial extent to approximately 0.15 mm in the burning direction. The aperture between the sample and the spectrometer minimizes collection of emission signal and the 10 cm focal length cylindrical lens (CYL1) focusses the transmitted light onto the spectrometer entrance slit. Aperture sizes (A) between 0.5 and 1.0 mm were used to keep the emission signal levels to less than 2% of the absorption signal. In actuality the aperture size was set from the results obtained from a  $\text{CH}_4/\text{N}_2\text{O}$  flame, and it was assumed that the propellant would be similar in this respect. The spectrometer has a 0.3 m focal length and a 2400 groove per mm grating which when operated second order gave a spectral resolution of about 0.03 nm with a 0.025 mm entrance slit. This system allows a 6 nm band of light to be sampled at one time on the intensified photodiode array. A uv transmitting black glass filter (Schott UG-11) eliminated first order light from entering the spectrometer. OH rotational absorptions of interest are much narrower than this 6 nm band; thus intensities of wavelengths which undergo absorption, and nearby wavelengths which do not, can be recorded simultaneously. The system therefore provides a simple calibration of effective incident intensity in cases where continuous absorbers or scatterers interfere.

Two combustion systems have been experimentally studied: a premixed  $\text{CH}_4/\text{N}_2\text{O}$  flame and a solid propellant flame. The solid propellant (HMX1)<sup>2</sup> is composed of 73% cyclotetramethylenetetranitramine (HMX). The  $\text{CH}_4/\text{N}_2\text{O}$  flame has been used primarily for calibration and comparison purposes where a path length has been chosen similar to the path length used for the propellant absorption studies. A burner consisting of many small holes within a 0.4 cm diameter (the path length) was used to support this premixed flame. The top of the combustion vessel is removable and thus this flame can be placed at the sample location for experimentation. Long path lengths are traditionally desirable for trace species since, for small absorptions, the absorption increases linearly with path length. However, in these studies the overriding concern was to produce a horizontal burning propellant surface, i.e., a surface which is parallel to the direction of the arc lamp light beam. This condition could only be obtained for small cross sections. An HMX1 propellant geometry which exhibited a reasonable cigarette fashion burn and was thus used, was a strand about 4 cm long with an octagonal cross section that measured 0.65 cm between opposing faces. The propellant strand was coated with a thin layer of fingernail polish to inhibit side burning.

A partial diagram of the windowed combustion vessel is shown in cross section on Fig. 1. This vessel is made from stainless steel with two pairs of opposing windows and provides an environment to burn propellants at an elevated pressure. An exit orifice in the vessel allows a purge gas to be flowed at rates typically about four times the propellant gasification rate. A video camera (not shown) provides a photographic record of each propellant burn. This record provides the burning rate of the propellant as well as visual information on the "flatness" of burn. Further details of the combustion vessel can be found elsewhere.<sup>3,4</sup>

Propellant burning in this experiment is a transient process since the burning surface regresses with time. This limits the amount of time that data can be taken depending on the amount of spatial resolution desired. The first studies of OH in a propellant produced marginally acceptable data and thus a propellant feed mechanism was incorporated into the

experiment to expand the data acquisition time. A sketch of the feed mechanism is shown on Fig. 2. This mechanism is more rudimentary than previous feed mechanisms<sup>5,6</sup> in several respects. First, the feed mechanism is not enclosed in the pressure vessel, but rather couples in linear motion by a drive shaft sealed with a plastic ferrule swage. Second, the drive shaft is unidirectional during the experiment with the feed rate and travel distance having been programmed into the speed control. Instead of maintaining an optical feedback control, the feed rate is set to be some large fraction of the propellant burn rate. For the experiments reported here the speed controller was programmed to drive the translator at a linear rate of 1.00 mm/s. The apparent burn rate, as viewed by a video camera, was measured as 0.27 mm/s which means the actual burn rate of HMX1 in a combustion vessel pressurized to 1.5 MPa nitrogen is 1.27 mm/s.

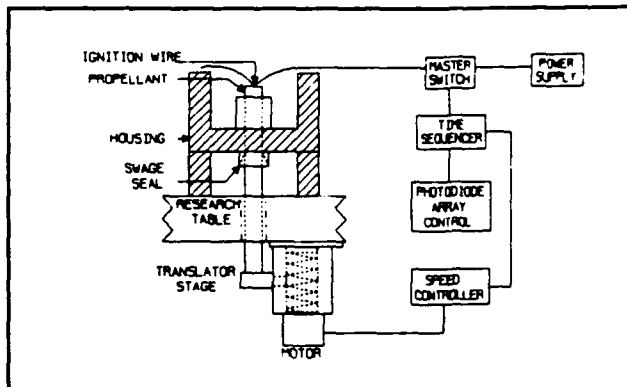


Figure 2 A sketch of the major components of the propellant feed mechanism and associated components that are triggered at various times during the course of an experimental run.

The following sequence of events occur for a typical propellant burn experiment. The combustion vessel is pressurized to 1.5 MPa nitrogen and the video recording system is activated. A master switch engages the power to heat the ignition wire and also starts the time sequencer. After preset delays the time sequencer starts the propellant feed and triggers the photodiode array control. The apertured light from the arc lamp is terminated by the propellant strand at the beginning of each experiment and the initial passage of this light to the detector indicates when the propellant surface is in the sampling region. The photodiode array repetitively scans and resets many times while storing each scan into buffer memory. The total data accumulation time as well as the time for each scan can be varied over a wide range. Total data accumulation times were major fractions of the total propellant burn time, ranging from 15 to 20 seconds.

### III. DATA ANALYSIS

In this section working equations are presented which are used to extract temperatures and absolute concentrations from experimental absorption spectra. The development and detailed discussions of these equations can be found elsewhere.<sup>7,8</sup> Based on the differential absorption law for a parallel beam of light of frequency  $\nu$  traveling in the  $+x$  direction through a medium with absorption coefficient  $k(\nu)$ ,

$$-dI = I k(\nu) dx ,$$

the intensity of the incident beam,  $I_0$  (assumed to be constant), is attenuated along a path of length  $\ell$  according to

$$I(\nu) = I_0 \exp[-\ell k(\nu)] .$$

Assuming a Boltzmann distribution the transmitted intensity of a group of lines is given by

$$I(\nu) = I_0 \exp\{-(h\nu l/c) [N_T/Q(T)] [\sum_j B_j g_j \exp(-E_j/kT) P_j(\nu)]\},$$

where  $h$  is Planck's constant,  $c$  is the speed of light,  $k$  is the Boltzmann constant,  $T$  is the absolute temperature,  $B_j$  is the absolute Einstein coefficient of absorption for the  $j$ th transition in energy density units,  $g_j$  is the degeneracy of the  $j$ th sublevel and  $E_j$  its energy.  $N_T$  is the total number density,  $Q(T)$  is the partition function which is evaluated using a standard closed form expression, and  $P_j$  is the transition lineshape. For conditions where the light source and spectrometer bandwidth is much larger than the width of a typical absorption line, an instrument function,  $S(\nu, \nu_0)$ , centered at  $\nu_0$  and normalized to unit area is introduced to give

$$I_{tr} = \int S(\nu, \nu_0) I(\nu) d\nu,$$

where  $I_{tr}$  is the integrated light transmitted.

The Einstein coefficients for OH are from Dimpfl and Kinsey<sup>9</sup> and the transition frequencies are from Dieke and Crosswhite<sup>10</sup>. 126 transitions of the A-X (0,0) band are included in the calculation, although typically only 90 are used for the range of data selected for analysis. Other molecule specific parameters are from Huber and Herzberg<sup>11</sup>. A multiparameter, nonlinear, least squares program with interactive graphics running on a 386/25MHz PC was used to fit the data. Since the width of the instrument function, taken to be Lorentzian, is larger than the transition linewidth, and in order to reduce computation time, the transition lineshape was approximated as a delta-function, thereby reducing the above integral to a sum. Using this model, the time to fit a spectrum was 10 minutes or less. Further details about the fitting procedure are found in the Appendix.

#### IV. RESULTS

Previously<sup>4</sup>, OH concentrations for an HMX propellant have been computed from peak absorptions of the Q<sub>2</sub> bandhead in the A-X (0,0) vibrational band system for OH. There the experimental data were not sufficiently resolved for the determination of temperature and thus it was necessary to construct a temperature profile by other means<sup>4</sup>. Only for a CH<sub>4</sub>/N<sub>2</sub>O flame were the data of sufficient quality to calculate a temperature from a Boltzmann plot<sup>4</sup>. We report here simultaneous temperature and concentration determinations for both a steady state CH<sub>4</sub>/N<sub>2</sub>O flame and a solid propellant flame. An example OH

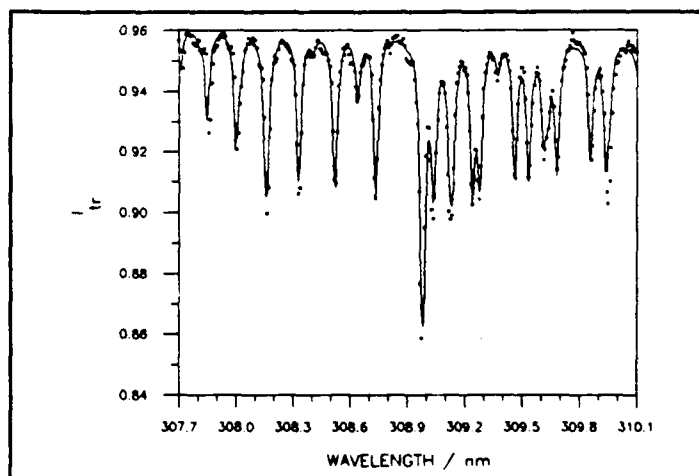


Figure 3 Absorption spectrum of the A-X (0,0) band system of OH, taken 1 mm above the burner surface of a premixed CH<sub>4</sub>/N<sub>2</sub>O flame. (●) is the data and the solid line is the least squares fit.

absorption spectrum, taken in a  $\text{CH}_4/\text{N}_2\text{O}$  flame at atmospheric pressure, is shown in Fig. 3. The absorption path length for this flame was 0.4 cm and one second was required to obtain the data. All of the absorptions observed experimentally on Fig. 3 are accounted for by the fitting program. Thus there is reasonable confidence that the discrete absorptions over the wavelength range from 307.7 to 310.1 nm are due solely to OH. A value of 2367 K has been determined for the temperature of this small premixed flame. All least squares fitted values and the standard deviations are given in Table 1. This value is in good agreement with prior determinations<sup>4</sup> of temperature for this flame which gave 2360 K and 2304 K obtained from Boltzmann plots of peak rotational values for OH emission and absorption, respectively. The adiabatic flame temperature for a stoichiometric  $\text{CH}_4/\text{N}_2\text{O}$  flame is 2922 K; however, this flame was strongly burner stabilized and, as has been found with other burner stabilized flames<sup>12</sup>, can have substantial heat loss to the burner head. Although the purpose of using a small steady state flame was only for setting up for propellant measurements, the absolute concentration determination for OH agrees well with published trends. That is, the fitted value of  $3.9 \times 10^{16}$  molecules/cc is about 1.7 times larger than the thermochemical equilibrium value<sup>13</sup> and is very similar (1.5 times) to the peak concentration of OH<sup>12</sup> reported for a stoichiometric  $\text{CH}_4/\text{N}_2\text{O}$  flame operating at atmospheric pressure.

Sample OH absorption data together with the least squares fit for an HMX1 propellant sample burning in 1.5 MPa nitrogen are shown on Fig. 4. The fitted values for the spectrum of Fig. 4 and for eight other spectra at different positions from the propellant surface are tabulated in Table 1. It was necessary to accumulate data for times corresponding to movement of the propellant surface in order to obtain statistically reasonable data; hence the propellant spectrum of Fig. 4 is an average over 0.4 mm. Here again for the propellant case all of the prominent features over the wavelength range from 307.9 to 310.3 nm have been accounted for with the OH fitting program. Temperatures and OH concentrations with their standard deviations have been tabulated in Table 1 and are plotted on Figs. 5 and 6. The temperature rise from the propellant surface to the final flame temperature occurs within 0.4 mm of the propellant surface. Within the statistical uncertainty of the data the fitted temperature reaches the adiabatic flame temperature. It also appears from Fig. 5 that the temperature is slightly dropping with increasing distance from the propellant surface. These temperature measurements can be directly compared with the recent results obtained by Stufflebeam and Eckbreth<sup>14</sup>. Using a CARS technique they have measured temperatures in HMX1 propellants burning in 2.31 MPa helium. Values ranging from 2600 K at 2.4 mm from the propellant surface to 1900 K at 12 mm from the surface were observed. The present data are in

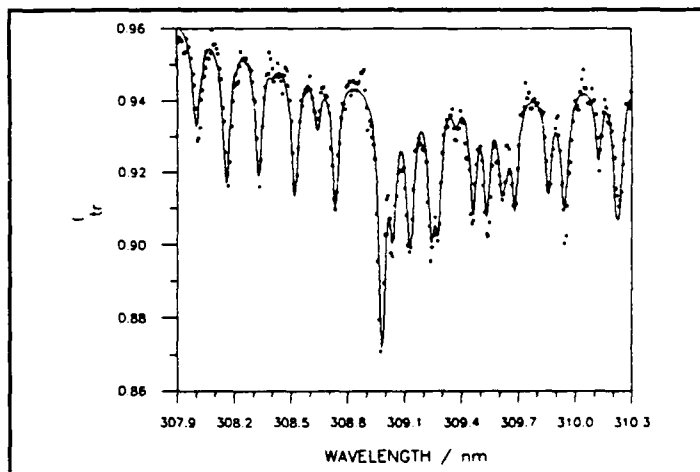


Figure 4 Same as Fig. 3 except here the sample is an HMX1 propellant burning in 1.5 MPa  $\text{N}_2$  from 0.4 to 0.9 mm above the propellant surface, corresponding to a data acquisition time of 1.6 seconds.

excellent agreement with these published results.

OH concentrations as a function of distance from the propellant surface are shown on Fig. 6. A rise in OH concentration can be observed at distances less than about 1 mm from the propellant surface and the concentration decreases further from the propellant surface due to cooling of the flame. Together with these data are dashed lines which represent calculated OH concentrations assuming thermochemical equilibrium. The three concentrations computed are for temperatures of 2617 (adiabatic), 2500 and 2400 K. Thus it is seen from Fig. 6 that the OH concentrations computed

from fitting OH absorption spectra fall in a thermochemical equilibrium concentration range from slightly above 2500 K to about 2400 K. Although the standard deviation in the OH concentration determinations do not allow for concentrations high enough to satisfy an adiabatic flame temperature, the total error in the OH concentration determination is estimated to be a factor of two. This additional uncertainty comes from the path length and

Table 1 Temperature and OH concentration values and standard deviations obtained from fitting OH absorption spectra.

System	Distance	Temperature	OH Concentration
	mm	K	$10^{16}$ molecules/cc
CH / N O 4 2	1	2356(124)	3.9(0.2)
HMX1	0 - 0.4	2739(281)	1.5(0.2)
	0.4 - 0.9	2512(115)	2.5(0.1)
	0.9 - 1.8	2690(116)	2.8(0.2)
	1.8 - 2.7	2540(103)	2.7(0.1)
	2.7 - 3.6	2479(114)	2.2(0.1)
	3.6 - 4.5	2704(131)	2.2(0.1)
	4.5 - 5.4	2038(103)	1.6(0.1)
	5.4 - 6.3	2290(107)	1.7(0.1)
	6.3 - 7.2	2437(176)	1.2(0.1)

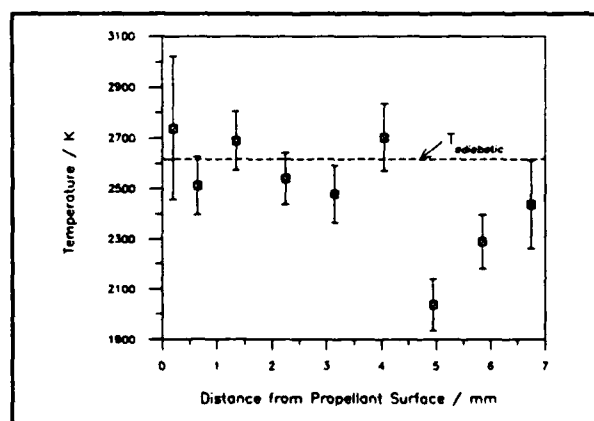


Figure 5 Temperature as a function of distance from the propellant surface for an HMX1 propellant burning in 1.5 MPa nitrogen. (●) represent the temperature data which is tabulated in Table 1.

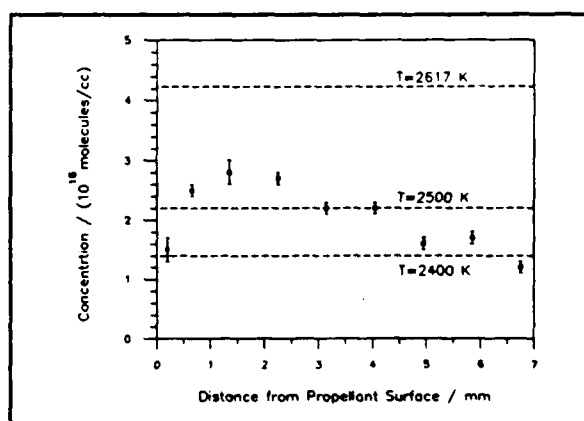


Figure 6 Concentration as a function of distance from the propellant surface corresponding to the temperatures in Fig. 5.



lineshape variables which affect the concentration determination much more than the temperature. A factor of two uncertainty in experimental OH concentration does include the computed OH equilibrium concentrations appropriate for the adiabatic flame temperature. There is no known direct comparisons for absolute OH concentrations measured in a solid propellant flame except for some of our previous work<sup>4</sup> using only a peak absorption of the Q<sub>2</sub> bandhead at 309 nm. Here concentrations for OH in HMX1 burning in 1.5 MPa nitrogen were about a factor of two smaller than those presented here. The difference in these results is primarily the result of using a Lorentzian instrument function for the present study, rather than the triangular function previously used.

## V. SUMMARY

Temperature and OH concentration profiles have been obtained for a solid propellant burning at elevated pressure using a sensitive absorption technique together with least squares fitting of a number of rotationally resolved lines. The rather coarse spatial resolution of 0.4 mm compromised the ability to observe the initial rise in temperature and OH concentration however, because OH varies slowly in comparison to many other radical species (after this initial rise), it is believed that the rest of the profile is adequately represented. Both the temperature and concentrations obtained are consistent with this solid propellant flame burning at its adiabatic flame temperature, and an OH concentration in thermochemical equilibrium.

INTENTIONALLY LEFT BLANK.

## REFERENCES

1. Lempert, W. R.: *Microwave Resonance Lamp Absorption Technique for Measuring Temperature and OH Number Density in Combustion Environments*, Combust. Flame, **73**, 89 (1988).
2. Edwards, J. T.: *Solid Propellant Flame Spectroscopy*, AFAL-TR-88-076, 1988.
3. Vanderhoff, J. A.: *Spectral Studies of Propellant Combustion: Experimental Details and Emission Results for M-30 Propellant*, BRL-MR-3714, 1988.
4. Vanderhoff, J. A.: *Spectral Studies of Solid Propellant Combustion II. Emission and Absorption Results for M-30 and HMX1 Propellants*, BRL-TR-3055, 1989.
5. Rekers, R. G. and Villars, D. S.: *Flame Zone Spectroscopy of Solid Propellants*, Rev. Sci. Instrum., **25**, 424 (1954).
6. Edwards, T. J., Weaver, D. P., Adams, R., Hulsizer, S., and Campbell, D. H.: *High-Pressure Combustor for the Spectroscopic Study of Solid Propellant Combustion Chemistry*, Rev. Sci. Instrum., **56**, 2131 (1985).
7. Mitchell, A. C. G. and Zemansky, M. W.: *Resonance Radiation and Excited Atoms*, Cambridge University Press, 1971.
8. Lucht, R. P., Peterson, R. C. and Laurendeau, N. M.: *Fundamentals of Absorption Spectroscopy for Selected Diatomic Flame Radicals*, PURDU-CL-78-06, 1978.
9. Dimpfl, W. L. and Kinsey, J. L.: *Radiative Lifetimes of OH ( $A^2\Sigma$ ) and Einstein Coefficients for the A-X System of OH and OD*, J. Quant. Spec. Radiat. Transfer, **21**, 233 (1979).
10. Dieke, G. AND Crosswhite, H.: *The Ultraviolet Bands of OH: Fundamental Data*, J. Quant. Spec. Radiat. Transfer, **2**, 97, (1963).
11. Huber, K. P., and Herzberg, G.: *Molecular Spectra and Molecular Structure. IV. Constants of Diatomic Molecules*, Van Nostrand Reinhold Company, 1979.
12. Anderson, W. R., Decker, L. J., and Kotlar, A. J.: *Temperature Profile of a Stoichiometric  $CH_4/N_2O$  Flame from Laser Excited Fluorescence Measurements on OH*, Combust. Flame, **48**, 163 (1982).
13. Svehla, R. A. and McBride, B. J.: *Fortran IV Computer Program for Calculation of Thermodynamic and Transport Properties of Complex Chemical Systems*, NASA-TND-7056, 1973.
14. Stufflebeam, J. H. and Eckbreth, A. C.: *CARS Measurements of High Pressure Solid Propellant Combustion*, Combust. Sci. Technol., **66**, 163, (1989).

INTENTIONALLY LEFT BLANK.

## APPENDIX

Comparison using delta-function or Voigt lineshapes for fitting OH experimental spectra.

INTENTIONALLY LEFT BLANK.

## APPENDIX

Comparison using delta-function or Voigt lineshapes for fitting OH experimental spectra.

In order to verify the validity of using the delta-function approximation for the transition lineshapes, a typical flame spectrum was fitted using both the delta-function and a Voigt lineshape for the transitions. The comparison of the parameters that were determined or fixed in the fit is given in Table 2. The parameters in Table 2 with standard deviations ( $\pm 1\sigma$ ) are those that were allowed to float during the fit. Seven parameters were fitted

**Table 2** Comparison obtained from fitting a typical flame spectrum using either a Voigt or a delta-function transition lineshape.

NAME	VOIGT LINESHAPE		DELTA-FUNCTION LINESHAPE		DIFFERENCE
	FINAL VALUE	STANDARD DEVIATION	FINAL VALUE	STANDARD DEVIATION	
TEMP	2220.86343	90.74400	2262.57580	92.97000	1.8782%
NTOT	3.91337E+16	1.50E+15	3.73733E+16	1.51E+15	-4.4986%
RCH	550.83341	0.04223	550.82424	0.04242	-0.0017%
RLAM	3089.80000		3089.80000		
INC	0.07514	3.624E-5	0.07514	3.669E-5	0.0009%
SLIT	0.26855	0.00110	0.28312	0.00441	5.4253%
LGTH	0.40000		0.40000		
A0	0.96647	0.00164	0.96616	0.00165	-0.0323%
A1	-1.43822E-5	2.900E-6	-1.45467E-5	2.943E-6	1.1438%
TAU	0.17963	0.01727	N/A		
RERR	1.00000E-4		N/A		
STD	0.00502		0.00508		
XMIN	3077.33927		3077.33941		0.0000%
XMAX	3104.01394		3104.01528		0.0000%
time	~4-8 hrs.		~1 min.		

\* The parameter names used in the fitting program are retained in this table: TEMP, temperature (K); NTOT, total number density (molecules/cc); RCH, reference channel corresponding to RLAM, reference wavelength (Å); INC, wavelength increment per channel (Å); SLIT, instrument function FWHM (Å); LGTH, absorption pathlength (cm); A0 and A1, constant and first order baseline coefficients; TAU, Lorentzian FWHM (cm<sup>-1</sup>); RERR, relative error of the numerical integration; STD, standard deviation of the fit; XMIN and XMAX, minimum and maximum wavelength (Å) of the fitted portion of the spectrum. The approximate time for one iteration of the fit is also given.

using the delta-function lineshape; an additional parameter, the Lorentzian linewidth of the Voigt profile, TAU, was also fitted when a Voigt lineshape was used for the transitions. Of the seven common parameters fitted in both cases, the two of primary interest are the temperature, TEMP, and the total number density, NTOT. The other five parameters are related to the particular conditions under which the experiment was performed. The largest differences are associated with those parameters most closely dependent on the value of the transition linewidth, i.e. the width of the instrument function (SLIT) and the total number density. The differences in these parameters obtained using the computationally less demanding delta-function lineshape as opposed to the more accurate Voigt lineshape are ca. 5% and -4% respectively. A single temperature is obtained from the fit using the Voigt profile since both the rotational temperature, and the translational temperature which

determines the Doppler width in the Voigt profile, are assumed to be the same value; also, the pressure broadened (Lorentzian) linewidth is assumed to be the same for all the rotational lines. The approximate time of a least squares iteration for each model is also give in Table 2. Since typically 5-10 iterations are needed to refine a fit, the desirability of using the delta-function model for routine data analysis is apparent.



No of Copies	Organization	No of Copies	Organization
1	Office of the Secretary of Defense OUSD(A) Director, Live Fire Testing ATTN: James F. O'Bryon Washington, DC 20301-3110	1	Director US Army Aviation Research and Technology Activity Ames Research Center Moffett Field, CA 94035-1099
2	Administrator Defense Technical Info Center ATTN: DTIC-DDA Cameron Station Alexandria, VA 22304-6145	1	Commander US Army Missile Command ATTN: AMSMI-RD-CS-R (DOC) Redstone Arsenal, AL 35898-5010
1	HQDA (SARD-TR) WASH DC 20310-0001	1	Commander US Army Tank-Automotive Command ATTN: AMSTA-TSL (Technical Library) Warren, MI 48397-5000
1	Commander US Army Materiel Command ATTN: AMCDRA-ST 5001 Eisenhower Avenue Alexandria, VA 22333-0001	1	Director US Army TRADOC Analysis Command ATTN: ATAA-SL White Sands Missile Range, NM 88002-5502
1	Commander US Army Laboratory Command ATTN: AMSLC-DL Adelphi, MD 20783-1145	(Class. only) 1	Commandant US Army Infantry School ATTN: ATSH-CD (Security Mgr.) Fort Benning, GA 31905-5660
2	Commander US Army, ARDEC ATTN: SMCAR-IMI-I Picatinny Arsenal, NJ 07806-5000	(Unclass. only) 1	Commandant US Army Infantry School ATTN: ATSH-CD-CSO-OR Fort Benning, GA 31905-5660
2	Commander US Army, ARDEC ATTN: SMCAR-TDC Picatinny Arsenal, NJ 07806-5000	1	Air Force Armament Laboratory ATTN: AFATL/DLODL Eglin AFB, FL 32542-5000  <u>Aberdeen Proving Ground</u>
1	Director Benet Weapons Laboratory US Army, ARDEC ATTN: SMCAR-CCB-TL Watervliet, NY 12189-4050	2	Dir, USAMSAA ATTN: AMXSY-D AMXSY-MP, H. Cohen
1	Commander US Army Armament, Munitions and Chemical Command ATTN: SMCAR-ESP-L Rock Island, IL 61299-5000	1	Cdr, USATECOM ATTN: AMSTE-TD
1	Commander US Army Aviation Systems Command ATTN: AMSAV-DACL 4300 Goodfellow Blvd. St. Louis, MO 63120-1798	3	Cdr, CRDEC, AMCCOM ATTN: SMCCR-RSP-A SMCCR-MU SMCCR-MSI
		1	Dir, VLAMO ATTN: AMSLC-VL-D

<u>No. of Copies</u>	<u>Organization</u>
4	<p>Commander US Army Research Office ATTN: R. Ghirardelli D. Mann R. Singleton R. Shaw P.O. Box 12211 Research Triangle Park, NC 27709-2211</p>
2	<p>Commander Armament RD&amp;E Center US Army AMCCOM ATTN: SMCAR-AEE-B, D.S. Downs SMCAR-AEE, J.A. Lannon Picatinny Arsenal, NJ 07806-5000</p>
1	<p>Commander Armament RD&amp;E Center US Army AMCCOM ATTN: SMCAR-AEE-BR, L. Harris Picatinny Arsenal, NJ 07806-5000</p>
2	<p>Commander US Army Missile Command ATTN: AMSMI-RK, D.J. Ifshin W. Wharton Redstone Arsenal, AL 35898</p>
1	<p>Commander US Army Missile Command ATTN: AMSMI-RKA, A.R. Maykut Redstone Arsenal, AL 35898-5249</p>
1	<p>Office of Naval Research Department of the Navy ATTN: R.S. Miller, Code 432 800 N. Quincy Street Arlington, VA 22217</p>
1	<p>Commander Naval Air Systems Command ATTN: J. Ramnarace, AIR-54111C Washington, DC 20360</p>
1	<p>Commander Naval Surface Warfare Center ATTN: J.L. East, Jr., G-23 Dahlgren, VA 22448-5000</p>

<u>No. of Copies</u>	<u>Organization</u>
2	<p>Commander Naval Surface Warfare Center ATTN: R. Bernecker, R-13 G.B. Wilmot, R-16 Silver Spring, MD 20902-5000</p>
5	<p>Commander Naval Research Laboratory ATTN: M.C. Lin J. McDonald E. Oran J. Shnur R.J. Doyle, Code 6110 Washington, DC 20375</p>
1	<p>Commanding Officer Naval Underwater Systems Center Weapons Dept. ATTN: R.S. Lazar/Code 36301 Newport, RI 02840</p>
2	<p>Commander Naval Weapons Center ATTN: T. Boggs, Code 388 T. Parr, Code 3895 China Lake, CA 93555-6001</p>
1	<p>Superintendent Naval Postgraduate School Dept. of Aeronautics ATTN: D.W. Netzer Monterey, CA 93940</p>
4	<p>AL/LSCF ATTN: R. Corley R. Geisler J. Levine Edwards AFB, CA 93523-5000</p>
1	<p>AL/MKPB ATTN: B. Goshgarian Edwards AFB, CA 93523-5000</p>
1	<p>AFOSR ATTN: J.M. Tishkoff Bolling Air Force Base Washington, DC 20332</p>
1	<p>OSD/SDIO/UST ATTN: L. Caveny Pentagon Washington, DC 20301-7100</p>

<u>No. of Copies</u>	<u>Organization</u>	<u>No. of Copies</u>	<u>Organization</u>
1	Commandant USAFAS ATTN: ATSF-TSM-CN Fort Sill, OK 73503-5600	1	AVCO Everett Research Laboratory Division ATTN: D. Stickler 2385 Revere Beach Parkway Everett, MA 02149
1	FJ. Seiler ATTN: S.A. Shackelford USAF Academy, CO 80840-6528	1	Battelle Memorial Institute Tactical Technology Center ATTN: J. Huggins 505 King Avenue Columbus, OH 43201
1	University of Dayton Research Institute ATTN: D. Campbell AL/PAP Edwards AFB, CA 93523	1	Cohen Professional Services ATTN: N.S. Cohen 141 Channing Street Redlands, CA 92373
1	NASA Langley Research Center Langley Station ATTN: G.B. Northam/MS 168 Hampton, VA 23365	1	Exxon Research & Eng. Co. ATTN: A. Dean Route 22E Annandale, NJ 08801
4	National Bureau of Standards ATTN: J. Hastie M. Jacox T. Kashiwagi H. Semerjian US Department of Commerce Washington, DC 20234	1	Ford Aerospace and Communications Corp. DIVAD Division Div. Hq., Irvine ATTN: D. Williams Main Street & Ford Road Newport Beach, CA 92663
1	Aerojet Solid Propulsion Co. ATTN: P. Micheli Sacramento, GA 95813	1	General Applied Science Laboratories, Inc. 77 Raynor Avenue Ronkonkoma, NY 11779-6649
1	Applied Combustion Technology, Inc. ATTN: A.M. Varney P.O. Box 17885 Orlando, FL 32860	1	General Electric Armament & Electrical Systems ATTN: M.J. Bulman Lakeside Avenue Burlington, VT 05401
2	Applied Mechanics Reviews The American Society of Mechanical Engineers ATTN: R.E. White A.B. Wenzel 345 E. 47th Street New York, NY 10017	1	General Electric Ordnance Systems ATTN: J. Mandzy 100 Plastics Avenue Pittsfield, MA 01203
1	Atlantic Research Corp. ATTN: M.K. King 5390 Cherokee Avenue Alexandria, VA 22314	2	General Motors Rsch Labs Physics Department ATTN: T. Sloan R. Teets Warren, MI 48090
1	Atlantic Research Corp. ATTN: R.H.W. Waesche 7511 Wellington Road Gainesville, VA 22065		

<u>No. of Copies</u>	<u>Organization</u>
2	Hercules, Inc. Allegheny Ballistics Lab. ATTN: W.B. Walkup E.A. Youn P.O. Box 210 Rocket Center, WV 26726
1	Honeywell, Inc. Government and Aerospace Products ATTN: D.E. Broden/ MS MN50-2000 600 2nd Street NE Hopkins, MN 55343
1	Honeywell, Inc. ATTN: R.E. Tompkins MN38-3300 10400 Yellow Circle Drive Minnetonka, MN 55345
1	IBM Corporation ATTN: A.C. Tam Research Division 5600 Cottle Road San Jose, CA 95193
1	IIT Research Institute ATTN: R.F. Remaly 10 West 35th Street Chicago, IL 60616
2	Director Lawrence Livermore National Laboratory ATTN: C. Westbrook M. Costantino P.O. Box 808 Livermore, CA 94550
1	Lockheed Missiles & Space Co. ATTN: George Lo 3251 Hanover Street Dept. 52-35/B204/2 Palo Alto, CA 94304
1	Los Alamos National Lab ATTN: B. Nichols T7, MS-B284 P.O. Box 1663 Los Alamos, NM 87545
1	National Science Foundation ATTN: A.B. Harvey Washington, DC 20550

<u>No. of Copies</u>	<u>Organization</u>
1	Olin Corporation Smokeless Powder Operations ATTN: V. McDonald P.O. Box 222 St. Marks, FL 32355
1	Paul Gough Associates, Inc. ATTN: P.S. Gough 1048 South Street Portsmouth, NH 03801-5423
2	Princeton Combustion Research Laboratories, Inc. ATTN: M. Summerfield N.A. Messina 475 US Highway One Monmouth Junction, NJ 08852
1	Hughes Aircraft Company ATTN: T.E. Ward 8433 Fallbrook Avenue Canoga Park, CA 91303
1	Rockwell International Corp. Rocketdyne Division ATTN: J.E. Flanagan/HB02 6633 Canoga Avenue Canoga Park, CA 91304
4	Sandia National Laboratories Division 8354 ATTN: R. Cattolica S. Johnston P. Mattern D. Stephenson Livermore, CA 94550
1	Science Applications, Inc. ATTN: R.B. Edelman 23146 Cumorah Crest Woodland Hills, CA 91364
3	SRI International ATTN: G. Smith D. Crosley D. Golden 333 Ravenswood Avenue Menlo Park, CA 94025
1	Stevens Institute of Tech. Davidson Laboratory ATTN: R. McAlevy, III Hoboken, NJ 07030

<u>No. of Copies</u>	<u>Organization</u>
1	Thiokol Corporation Elkton Division ATTN: S.F. Palopoli P.O. Box 241 Elkton, MD 21921
1	Morton Thiokol, Inc. Huntsville Division ATTN: J. Deur Huntsville, AL 35807-7501
3	Thiokol Corporation Wasatch Division ATTN: S.J. Bennett P.O. Box 524 Brigham City, UT 84302
1	United Technologies ATTN: A.C. Eckbreth East Hartford, CT 06108
3	United Technologies Corp. Chemical Systems Division ATTN: R.S. Brown T.D. Myers (2 copies) P.O. Box 9028 San Jose, CA 95151-9028
1	Universal Propulsion Company ATTN: H.J. McSpadden Black Canyon Stage 1 Box 1140 Phoenix, AZ 85029
1	Veritay Technology, Inc. ATTN: E.B. Fisher 4845 Millersport Highway P.O. Box 305 East Amherst, NY 14051-0305
1	Brigham Young University Dept. of Chemical Engineering ATTN: M.W. Beckstead Provo, UT 84601
1	California Institute of Tech. Jet Propulsion Laboratory ATTN: L. Strand/MS 512/102 4800 Oak Grove Drive Pasadena, CA 91009

<u>No. of Copies</u>	<u>Organization</u>
1	California Institute of Technology ATTN: F.E.C. Culick/ MC 301-46 204 Karman Lab. Pasadena, CA 91125
1	University of California, Berkeley Mechanical Engineering Dept. ATTN: J. Daily Berkeley, CA 94720
1	University of California Los Alamos Scientific Lab. P.O. Box 1663, Mail Stop B216 Los Alamos, NM 87545
1	University of California, San Diego ATTN: F.A. Williams AMES, B010 La Jolla, CA 92093
2	University of California, Santa Barbara Quantum Institute ATTN: K. Schofield M. Steinberg Santa Barbara, CA 93106
2	University of Southern California Dept. of Chemistry ATTN: S. Benson C. Wittig Los Angeles, CA 90007
1	Case Western Reserve Univ. Div. of Aerospace Sciences ATTN: J. Tien Cleveland, OH 44135
1	Cornell University Department of Chemistry ATTN: T.A. Cool Baker Laboratory Ithaca, NY 14853
1	University of Delaware ATTN: T. Brill Chemistry Department Newark, DE 19711

<u>No. of Copies</u>	<u>Organization</u>
1	University of Florida Dept. of Chemistry ATTN: J. Winefordner Gainesville, FL 32611
3	Georgia Institute of Technology School of Aerospace Engineering ATTN: E. Price W.C. Strahle B.T. Zinn Atlanta, GA 30332
1	University of Illinois Dept. of Mech. Eng. ATTN: H. Krier 144MEB, 1206 W. Green St. Urbana, IL 61801
1	Johns Hopkins University/APL Chemical Propulsion Information Agency ATTN: T.W. Christian Johns Hopkins Road Laurel, MD 20707
1	University of Michigan Gas Dynamics Lab Aerospace Engineering Bldg. ATTN: G.M. Faeth Ann Arbor, MI 48109-2140
1	University of Minnesota Dept. of Mechanical Engineering ATTN: E. Fletcher Minneapolis, MN 55455
3	Pennsylvania State University Applied Research Laboratory ATTN: K.K. Kuo H. Palmer M. Micci University Park, PA 16802
1	Pennsylvania State University Dept. of Mechanical Engineering ATTN: V. Yang University Park, PA 16802

<u>No. of Copies</u>	<u>Organization</u>
1	Polytechnic Institute of NY Graduate Center ATTN: S. Lederman Route 110 Farmingdale, NY 11735
2	Princeton University Forrestal Campus Library ATTN: K. Brezinsky I. Glassman P.O. Box 710 Princeton, NJ 08540
1	Purdue University School of Aeronautics and Astronautics ATTN: J.R. Osborn Grissom Hall West Lafayette, IN 47906
1	Purdue University Department of Chemistry ATTN: E. Grant West Lafayette, IN 47906
2	Purdue University School of Mechanical Engineering ATTN: N.M. Laurendeau S.N.B. Murthy TSPC Chaffee Hall West Lafayette, IN 47906
1	Rensselaer Polytechnic Inst. Dept. of Chemical Engineering ATTN: A. Fontijn Troy, NY 12181
1	Stanford University Dept. of Mechanical Engineering ATTN: R. Hanson Stanford, CA 94305
1	University of Texas Dept. of Chemistry ATTN: W. Gardiner Austin, TX 78712
1	University of Utah Dept. of Chemical Engineering ATTN: G. Flandro Salt Lake City, UT 84112

No. of  
Copies

Organization

No. of  
Copies

Organization

1 Virginia Polytechnic  
Institute and  
State University  
ATTN: J.A. Schetz  
Blacksburg, VA 24061

1 Freedman Associates  
ATTN: E. Freedman  
2411 Diana Road  
Baltimore, MD 21209-1525

INTENTIONALLY LEFT BLANK.



## USER EVALUATION SHEET/CHANGE OF ADDRESS

This Laboratory undertakes a continuing effort to improve the quality of the reports it publishes. Your comments/answers to the items/questions below will aid us in our efforts.

1. BRL Report Number BRL-TR-3098 Date of Report APRIL 1990

2. Date Report Received \_\_\_\_\_

3. Does this report satisfy a need? (Comment on purpose, related project, or other area of interest for which the report will be used.) \_\_\_\_\_  
\_\_\_\_\_  
\_\_\_\_\_

4. Specifically, how is the report being used? (Information source, design data, procedure, source of ideas, etc.) \_\_\_\_\_  
\_\_\_\_\_  
\_\_\_\_\_

5. Has the information in this report led to any quantitative savings as far as man-hours or dollars saved, operating costs avoided, or efficiencies achieved, etc? If so, please elaborate. \_\_\_\_\_  
\_\_\_\_\_  
\_\_\_\_\_

6. General Comments. What do you think should be changed to improve future reports? (Indicate changes to organization, technical content, format, etc.) \_\_\_\_\_  
\_\_\_\_\_  
\_\_\_\_\_  
\_\_\_\_\_

### CURRENT ADDRESS

\_\_\_\_\_  
Name

\_\_\_\_\_  
Organization

\_\_\_\_\_  
Address

\_\_\_\_\_  
City, State, Zip Code

7. If indicating a Change of Address or Address Correction, please provide the New or Correct Address in Block 6 above and the Old or Incorrect address below.

### OLD ADDRESS

\_\_\_\_\_  
Name

\_\_\_\_\_  
Organization

\_\_\_\_\_  
Address

\_\_\_\_\_  
City, State, Zip Code

(Remove this sheet, fold as indicated, staple or tape closed, and mail.)

-----FOLD HERE-----

**DEPARTMENT OF THE ARMY**

Director  
U.S. Army Ballistic Research Laboratory  
ATTN: SLCBR-DD-T  
Aberdeen Proving Ground, MD 21005-5066  
**OFFICIAL BUSINESS**



NO POSTAGE  
NECESSARY  
IF MAILED  
IN THE  
UNITED STATES

**BUSINESS REPLY MAIL**  
FIRST CLASS PERMIT No 0001, APG, MD

POSTAGE WILL BE PAID BY ADDRESSEE

Director  
U.S. Army Ballistic Research Laboratory  
ATTN: SLCBR-DD-T  
Aberdeen Proving Ground, MD 21005-9989

-----FOLD HERE-----